Journal of Nuclear Materials 601 (2024) 155301

Contents lists available at ScienceDirect

Journal of Nuclear Materials

journal homepage: www.elsevier.com/locate/jnucmat

Chromia-doped UO_2 fuel: An engineering model for chromium solubility and fission gas diffusivity

Giovanni Nicodemo [a], Giovanni Zullo [a], Fabiola Cappia [b], Paul Van Uffelen [c,*], Alejandra De Lara [d], Lelio Luzzi [a], Davide Pizzocri [a]

[a] Politecnico di Milano, Department of Energy, Nuclear Energy Division, Milan, Italy
[b] Idaho National Laboratory, Idaho Falls, United States of America
[c] European Commission, Joint Research Centre (JRC), Karlsruhe, Germany
[d] University of Cambridge, Department of Engineering, Cambridge, United Kingdom

ARTICLE INFO

Keywords:
Chromium-doped fuel
Solubility
Gas diffusivity
SCIANTIX
Fission gas behaviour

ABSTRACT

Increasing the average grain size of fuel pellets by doping them with chromium oxide is one strategy to improve oxide nuclear fuels performance. The promoted fission gas retention is thought to improve the performance of the fuel at high burnup. In this work, we review models for the solubility of chromium in UO_2, and the evolution of the chromium phases in the fuel matrix during irradiation. These models are implemented in SCIANTIX, an open-source mesoscale code describing inert gas behaviour in nuclear fuel. We adjusted the chromium solubility model keeping each parameter within its range of compatibility with experimental data, targeting a better representation of available electron probe microanalysis data of chromium content in fuel after irradiation. As for fission gas behaviour, we considered a physics-based description of the chromium impact on the fission gas diffusivity in fuel grains. The expression for the fission gas diffusivity in standard non-doped uranium oxide has been extended by introducing the impact of the concentration of defects introduced by interstitial oxygen excess representing the effect of chromium content in the fuel itself. A preliminary integral assessment of the proposed models has been carried out against the available experimental data.

1. Introduction

Accumulation of fission products, particularly fission gases, is among the primary causes limiting the performance of the UO_2 fuels due to deteriorating safety and operational margins at high burnup [1]. During the reactor operation, fission gases (mainly Xenon and Krypton) are generated in the fuel pellets and partly released into the free volume of the fuel rod. The accumulation of the released fission gases in the rod free volume leads to an increase in the rod internal pressure [2,3]. Meanwhile, the gap conductance lowers due to the poor conductivity of the gaseous fission products in comparison to the initial helium fill gas. This leads to higher fuel temperature and, consequently, higher Fission Gas Release (FGR), creating a feedback loop. Thus, FGR is a life-limiting factor for the fuel rod and is enhanced at extended burnup and during power ramps [3–7]. A possible solution for controlling the rising FGR with burnup consists in modifying the initial fuel microstructure during the manufacturing process by using some additives that promote the crystalline growth of the fuel grains during sintering [2]. Such alteration of the initial fuel microstructure modifies the diffusion phenomena inside the fuel pellets, leading to an increased effective retention of the fission gas.[1] Among the numerous additives considered [8], chromium oxide appears as one of the most promising, since most of the thermal-mechanical properties of the unirradiated Cr_2O_3-doped fuel are fundamentally the same as the UO_2 fuels, such as thermal diffusivity and melting temperature [9].

Besides the enhanced fission gas retention, the increased average grain size, which was detected up to 7 times greater than the undoped fuel one [10], i.e. up to 50 μm of grain radius, also leads to a reduction in the strength of the fuel, increasing the pellet-cladding mechanical inter-

* Corresponding author.
E-mail address: paul.van-uffelen@ec.europa.eu (P. Van Uffelen).

[1] Fission gas behaviour is the complex combination of several competing phenomena. It is known that by using a Cr-doped fuel, the net effect is increased gas retention, as the reduction of grain boundaries prevails the effect on intragranular gas diffusivity.

https://doi.org/10.1016/j.jnucmat.2024.155301
Received 22 March 2024; Received in revised form 6 June 2024; Accepted 18 July 2024
Available online 26 July 2024

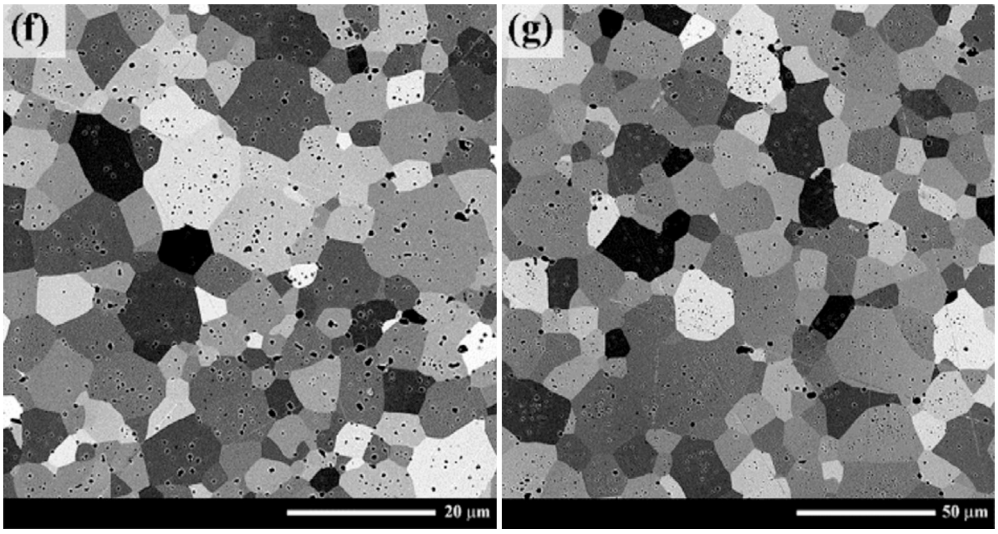

Fig. 1. Backscattering electron micrographs of the 1000 wppm Cr_2O_3-doped UO_2 samples heated at 1465 °C (f), and 1655 °C (g) temperatures for 10 h. The right figure shows the typical large grains that characterize chromium-doped fuels. Figure taken from the work by Silva et al. [10].

action (PCMI) margins [11]. An example of this modified microstructure is shown in Fig. 1.

During fabrication, chromium oxide is typically added, as a powder, to UO_2 powder in quantities of around ~1000 wt. ppm, which is then sintered at high temperature (1600–1800 °C) under a controlled atmosphere [12]. It is convenient to limit dopant content to the solubility limit to minimize the potential impact on other materials and neutronic fuel properties while maintaining the benefits of large grains. In fact, Chromium is a neutronic absorber, hence it could be combined with Aluminium, during the sintering process, to reduce this effect [13]. In this way, in the final product, chromium can be found mostly in a soluble fraction in the solid solution in UO_2 and, minimally, in an insoluble fraction as separate Cr oxide precipitates [14].

In this work, we review the chromium solubility model proposed by Riglet-Martial et al. [15], optimizing it to better reproduce available Electron Probe Microanalysis (EPMA) data [16], together with simple modelling of chromium phase evolution during irradiation based on the work by Curti and Kulik [17]. Then, a new description of the fission gas diffusion coefficient is derived, based on defect concentration induced by doping, consistent with the recent work by Murphy et al. [18].

All models are implemented in SCIANTIX, a meso scale 0D code [19] dedicated to a mechanistic description of fission gas behaviour. Lastly, a separate-effect comparison with experimental data is performed, for all models proposed. An integral assessment is discussed, considering results obtained with the Fuel Performance Code (FPC) TRANSURANUS [20] coupled with SCIANTIX [21].

2. Methods

2.1. Solubility and phase evolution models

A solubility model for Chromium in UO_2 was proposed by Riglet-Martial [15]. Due to the lack of experimental information in the literature in some key areas of the Cr - O phase diagram [22], additional measurements were collected by authors to obtain a full description of the system in the whole range of temperature and oxygen partial pressure P_{O_2} relevant to nuclear fuels. Four phases are highlighted in the phase diagram:

- $Cr_2O_{3(s)}$
- $Cr_3O_{4(s)}$
- $CrO_{(l)}$
- $Cr_{(s)}$

The phase $Cr_3O_{4(s)}$ is neglected since it is characterized by a small area in the phase diagram. In addition, authors also report that the $CrO_{(l)}$ phase (oxidation state +2) is still hardly evidenced, due to its narrow stability area only at high temperature. Moreover, experimental synthesis of pure $CrO_{(l)}$ phase encounters difficulties when trying to accurately adjust and maintain the sintering parameters during the whole process [15]. For these reasons, and since the stability region of $CrO_{(l)}$ is defined by conditions of oxygen potentials and temperature far from typical reactor operating conditions, this phase was neglected in the implementation of the solubility model in the SCIANTIX code.

As a result, a simplified solubility thermodynamic model has been developed combining all the relevant experimental data. The solubility law was obtained by thermodynamics considerations, leading to the following formula:

$$\log_{10}(y_{Cr}) = q \log_{10}(P_{O_2}) + V + \frac{U}{T} \tag{1}$$

where y_{Cr} is the chromium solubility, P_{O_2} is the oxygen partial pressure, T is the temperature, V and U are coefficients coming from the linearization of the Gibbs' free energy and q is a function of the stoichiometry of the soluble species. Coefficients were determined by fitting the experimental data, leading to solubility laws for oxide and metal phases as shown in Fig. 2.

The oxygen potential has a primary role in determining the stable chromium phase at a certain temperature. Few studies have been carried out to model from a thermo-chemical perspective and accounting for the FP evolution in the LWR fuel behaviour to determine oxygen potentials and its variation during irradiation [24] [25] [17]. In the last work, Curti and coauthors focus on the accurate thermodynamic description of chromium-doped fuel systems. The final model calculates complete thermodynamic equilibrium in a conventional or Cr-doped UO_2 fuel rod irradiated in a PWR, using detailed model inventories with a defined average burnup. It includes, besides stoichiometric solids and ideal gas, a complex UO_2 solution with U^{5+}, Cr^{3+}, Pu, minor actinides and lanthanides as minor solutes, a quinary (Mo, Pd, Rh, Ru, Tc) solid solution representing ϵ-particles, a binary (Ba, Sr)ZrO_3 solid solution representing a very simplified "grey phase" [17]. The main results of this work are the thermodynamic equilibrium calculations for PWR Cr-doped UO_2 fuel with 60 GWd/t_{HM} burnup.

Curti and coauthors found that, between 400 °C and 1400 °C, the speciation of chromium is dominated by a separate pure $Cr_2O_{3(cr)}$ phase. While, for higher temperatures, a phase transition between the oxide phase and the metal one is observed. The phase exchange between Cr - Cr_2O_3 was modelled with the following function

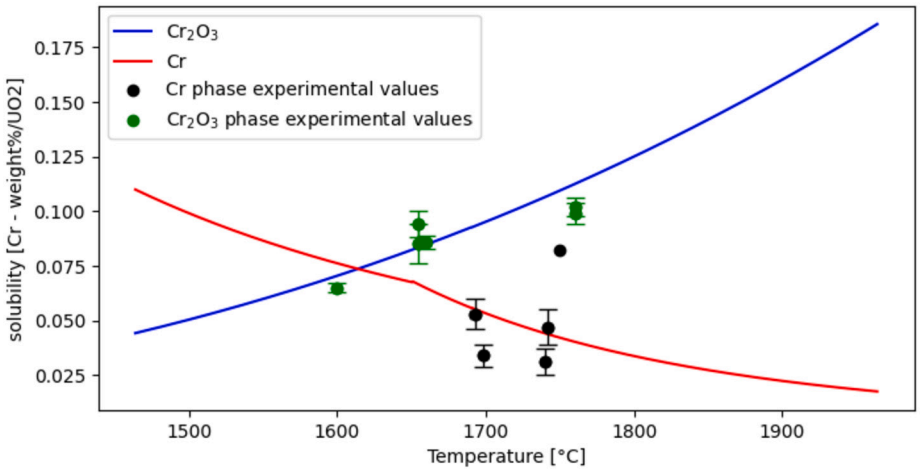

Fig. 2. Variation in the solubility of chromium in UO_2 as a function of the temperature: insoluble phase $Cr_2O_{3(sc)}$, in blue, and insoluble phase $Cr_{(sc)}$, in red. Experimental values, taken from the work of Riglet-Martial et al. [15], are reported in green for the $Cr_2O_{3(sc)}$ phase and in black for the $Cr_{(sc)}$ phase. Note that the highest value for the $Cr_{(sc)}$ solubility in UO_2 is reported without the error bars since it is old data by Une et al. [23]. The data point is reported for completeness, but the discrepancy from the larger data set from Riglet-Martial is obvious and might be considered an outlier. (For interpretation of the colours in the figure(s), the reader is referred to the web version of this article.)

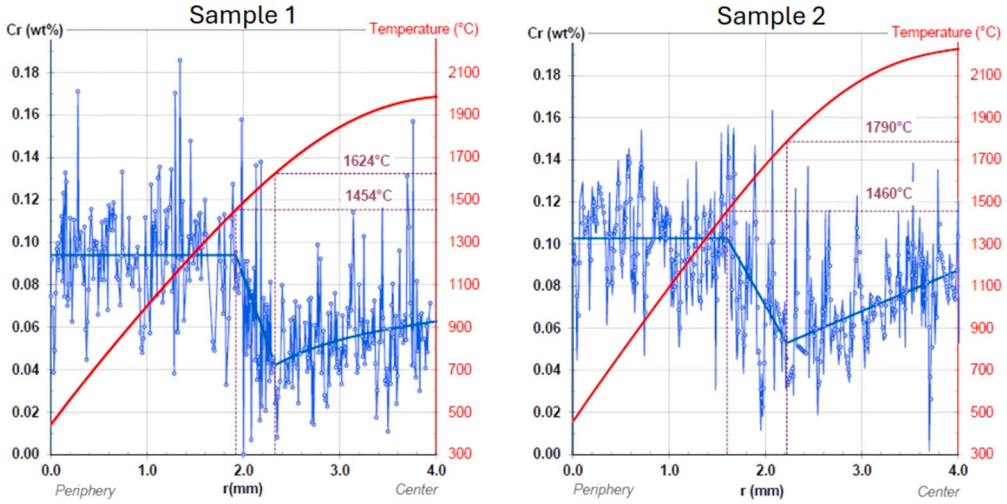

Fig. 3. Radial temperature profiles and concentration profiles of chromium measured by EPMA for the two ramp tests. On the left, sample one, undergoing a lower temperature ramp (up to ~ 2000 °C) and, on the right, sample two, undergoing the higher temperature ramp (up to ~ 2200 °C). Figure taken from the work by Riglet-Martial and coauthors [16].

$$f(T) = 1 - \exp(C_1(T - C_2)) \tag{2}$$

where C_1 and C_2 are appropriate coefficients, and f(T) describes the molar fraction of Cr; then the molar fraction of Cr_2O_3 is obtained by subtracting f(T) from 1. The effect of the burnup is taken into account considering that:

- An higher burnup and, thus, a higher production of FPs, would make the phase transition faster
- At the beginning of the irradiation life, the function should be a horizontal straight line since no phase transition is in place

In this way, it is possible to take into consideration how the presence of FPs can remove oxygen from chromium oxide molecules [26]. This is done by weighting the end-point of the function, represented by C_2, by the burnup. Thus Eq. (2) becomes:

$$\begin{cases} f(T,B) = 1 - \exp(C_1\ T - (C_2 - 400\ (B\text{-}60)/60)\ C_1) & B > 60 \\ f(T,B) = 1 - \exp(C_1\ T - (C_2 - 1000\ (B\text{-}60)/60)\ C_1) & B < 60 \end{cases} \tag{3}$$

where B is the burnup GWd/t_{HM}. The value of 60 GWd/t_{HM} is the same as reported by Curti and coauthors [17] in their equilibrium calculation and indicates how we vary the phase exchange function with respect to their calculations.

The chromium content in the UO_2 lattice depends on both phase distribution and solubility laws To increase the fidelity of the above-proposed models an optimization process was performed against experimental data by Riglet-Martial et al., [16], that are shown in Fig. 3. Only the solubility law of $Cr_{(sc)}$ was optimized, together with the phase-change function, since this law was obtained by less experimental data concentrated in a small temperature region. On the other hand, the solubility law for the oxide phase was considered reliable, given the greater availability of experimental data [12]. This optimization process aims to properly describe the amount of chromium in the lattice for different temperatures and burnup conditions. In addition, acting only on the U, and V parameters is possible to account for different fabrications that influence the oxygen partial pressure. From these results some conclusions can be drawn:

- In the low-temperature range of the pellet, between the periphery and the radial position that reached approximately a temperature value of 1400 °C, the soluble fraction of chromium in the UO_2 matrix is measured around a constant value of 0.1 wt% Cr, independent

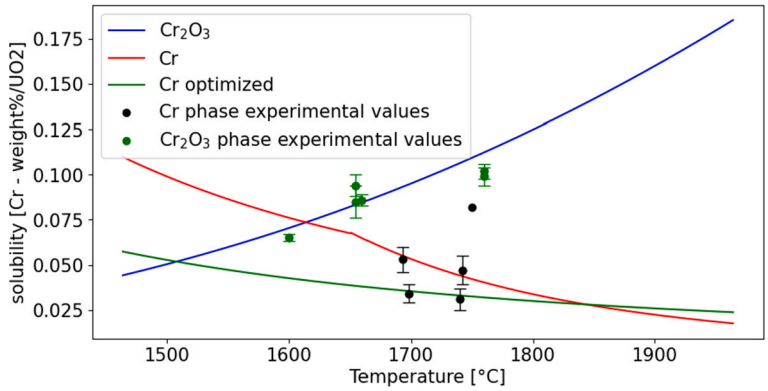

Fig. 4. Comparison between the solubility model from literature [15] and the optimized one against experimental data.

Table 1
Parameters value obtained from the optimization process compared with nominal ones. The U and V coefficients refer to the solubility law for the Cr metal phase.

Quantity	Nominal values	Optimized values
U (J/mol)	28160	22989.0
V (J/K mol)	-6.0760	-5.9483
C_1 (-)	0.0050	0.0017
C_2 (-)	1800	1502

of temperature. The chromium fraction in excess is found as precipitate in UO_2 as an oxide secondary phase. The chromium speciation (both soluble and insoluble forms) in the cold section of the rod is comparable to the one recorded on a pre-irradiated rod of the same type under nominal operating conditions (with temperatures between 500 °C and 1000 °C).

- In the intermediate-temperature range of the pellet, between the radial position that reached 1500 °C and the one that reached 1620 °C in sample 1 and 1790 °C in sample 2, the soluble fraction of chromium in UO_2 decreases significantly down to the range of 0.04 wt% - 0.06 wt% and, thus, abundant precipitation of metallic chromium is found as a secondary phase
- In the high-temperature range of the pellet, between the radial position that reached 1620 °C in sample 1 and 1790 °C in sample 2 and the centre of the pellet, the soluble fraction increases up to values in the range of 0.06 wt% - 0.09 wt%. Abundant precipitates are still observed.

It should be emphasized that the data are highly dispersed, and the considerations made about the average trend must take this uncertainty into account. This uncertainty is probably related to the experimental technique used for the experiment (EPMA), considering that the dopant concentration is quite low.

The aim was to reproduce the sudden decrease in the chromium content above ~1450 °C. Optimization was carried out only on the Cr phase, as this is the one for which less experimental data are available and about which there is therefore more uncertainty. Results are shown in Fig. 4.

The results obtained downstream of the optimization process suggest a faster transition between $Cr_2O_{3(sc)}$ and $Cr_{(sc)}$ and lower solubility of the $Cr_{(sc)}$ phase. Parameters of the optimized models are shown in Table 1.

2.2. Fission gas diffusivity model

FGR is a complex multi-step process [27] [28] [29] [30]:

1. FG is produced by fissions in the bulk UO_2 lattice, where unperturbed diffusion occurs.
2. trapping of the insoluble gas in intragranular bubbles and its resolution back into the lattice by irradiation occurs and can be assumed to rapidly reach equilibrium under most conditions of practical interest.
3. the resultant concentration of gas in the bulk diffuses to the grain boundaries (with the diffusion rate during equilibrium trapping and resolution captured by an effective diffusion coefficient) and forms inter-granular bubbles.
4. growth of the inter-granular bubbles leads to fuel swelling, bubble interconnection, and gas release upon the formation of percolating pathways to a free surface.

Due to considerations about chromium precipitates at the grain boundary, and considering that the probable chromium concentrations of commercial interest are rather low (~1000 - 1200 ppm) [10], the effect of precipitates on intragranular diffusion was neglected. It may be relevant only in the case of doping with large concentrations [31], consequently, the only effect related to grain boundaries is their reduction, since the doped fuel has larger grains. In this work the focus is on the intra-granular gas behaviour, which is controlled, among other factors, by the grain size and the gas diffusivity. The fission gas diffusivity for undoped UO_2 is given by the Turnbull model [32]:

$$D = D_1 + D_2 + D_3 \tag{4}$$

$$D_1 = 7.6 \cdot 10^{-10} \cdot \exp(-4.86 \cdot 10^{-19}/(k_B T)) \tag{5}$$

$$D_2 = 5.64 \cdot 10^{-25} \sqrt{\dot{F}} \cdot \exp(-1.91 \cdot 10^{-19}/(k_B T)) \tag{6}$$

$$D_3 = 8 \cdot 10^{-40} \dot{F} \tag{7}$$

where D_1, D_2, and D_3 represent the intrinsic, irradiation-enhanced, and athermal contributions to fission gas diffusivity, respectively [33]. According to the fact that the equilibrium between Cr_2O_3 and Cr occurs at an oxygen potential that is commensurate to a hyperstoichiometric UO_{2+x} fuel, as found in the work by Cooper [27], this formula was modified by adding a term accounting for uranium vacancy excess, retrieving a formulation discussed in many works, e.g. [32] [34]:

$$D_4 = h^2 \, j_V \, V_U \tag{8}$$

where h is the interatomic jump distance (m), j_V the vacancy jump rate (-), and V_U the vacancy induced by doping.[2] Assuming that Cr atoms enter interstitial sites in the UO_2 lattice and are ionized to a trivalency of +3, the lattice defect equilibrium is expressed by

[2] This is also how the stoichiometry deviation is treated in SCIANTIX, starting from the model from Carter and Lay [35] and Massih [36]. Thus, in this work, we neglect the effect of non-stoichiometry, which may be relevant if samples are non-perfectly stoichiometric because even very small deviations in stoichiometry can significantly impact uranium vacancy stability. This may also be related to the exact oxygen partial pressure during fabrication.

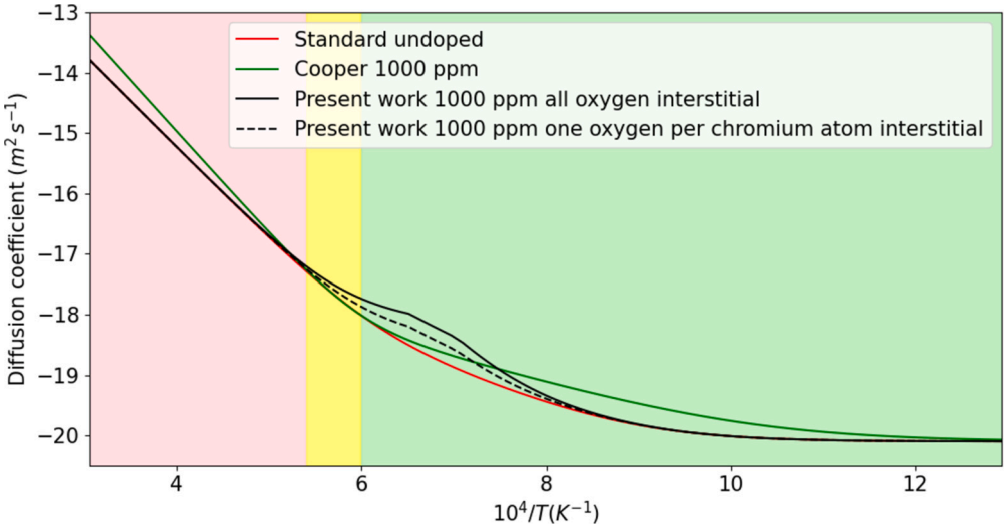

Fig. 5. Diffusion coefficients from this work, compared to the standard undoped one and the one derived by Cooper and coauthors [27]. It is highlighted the amount of chromium oxide, in wt ppm, used to dope the UO_2 fuel.

$$2Cr_i + 3/2O_2\ (gas) \longleftrightarrow 2\ Cr_i^{3+} + 3O_i^{2-} \tag{9}$$

Thus the concentration of O_i^{2-} interstitials is approximated by[3]

$$[O_i^{2-}] = \frac{3}{2}[Cr_i^{3+}] \tag{10}$$

When considering the Frenkel and Schottky equilibria, the following equations hold in the three kinds of defects of O_i, V_O and V_U:

$$[O_i][V_o] = K_1\ \text{(Frenkel defects)} \tag{11}$$

$$[V_o]^2[V_u] = K_2\ \text{(Schottky defects)} \tag{12}$$

where K_1 and K_2 are the equilibrium constants for the reactions of the defects. Hence, the uranium vacancy concentration is expressed by

$$[V_U] = \left(\frac{3}{2}\right)^2 \left(\frac{K_2}{K_1^2}\right)[Cr^{3+}]^2 \tag{13}$$

In which it is assumed that all the oxygen introduced as chromium-oxide in the fuel is retained in interstitial positions, leading to the formation of an equal number of oxygen vacancies. Another possibility, according to the work by Murphy et al. [18], is to consider one single oxygen vacancy per chromium atom in the lattice, leading to the following expression

$$[V_U] = \left(\frac{K_2}{K_1^2}\right)[Cr^{3+}]^2 \tag{14}$$

The results of calculations are shown in Fig. 5. It must be stated that the uncertainty associated with the intra-granular (lattice) gas atom diffusion coefficient appearing plays an important role in limiting the accuracy of Fission Gas behaviour (FGB) predictions. White and Tucker [7] postulated that the main cause of the observed discrepancies between the model and experiment in terms of FGR lay in the uncertainties in the lattice diffusion coefficients. Matzke [37] demonstrated a scatter of about two orders of magnitude, depending on the considered temperature, between different experimental data sets. In fact, a factor of 100 was considered also by Pastore and coauthors [38] to make a sensitivity analysis on FGR. Therefore, the comparison presented must be considered qualitatively, noting that the correction is considerable at intermediate temperatures and that it is associated with a physical process of creating uranium vacancies.

2.3. TRANSURANUS-SCIANTIX fuel performance simulations

Due to the relatively small concentration of chromium in UO_2 (~1000 wt. ppm), many standard undoped UO_2 properties are expected to remain similar in the doped UO_2. Arborelius et al. found that thermal properties are comparable to ones of undoped UO_2 [9]. Therefore standard TRANSURANUS model for thermal conductivity is considered [3]. Authors also note that Cr + Al-doped UO_2 has the same thermal expansion as UO_2 [9]. Therefore, the standard TRANSURANUS UO_2 thermal strain model [39] was adopted for Cr-doped UO_2. On the other hand, dedicated routines implemented in TRANSURANUS for Cr-doped UO2 were selected concerning the fuel cracking [40] and the thermal creep [41] [42]. In SCIANTIX, the grain growth of standard UO_2 due to the high temperatures can be characterised by selecting the grain growth model by Ainscough et al. [43] or the one by Van Uffelen et al. [44]. Moreover, these models contain parameters calibrated for non-doped small-grain fuel and, in addition, both models would not lead to significant grain growth due to the large initial grain size of doped UO_2 (~40–70 μm). This behaviour is expected due to the stability of large grains. For this reason, it was decided to not consider them. Thus, the simulation considered constant-size fuel grains, neglecting the grain growth.

As for the other SCIANTIX settings, the standard ones are used, except for the chromium solubility and the fission gas diffusion coefficient, for which the models developed in this work are considered.

3. Results

3.1. Separate-effect experiments

In this section, results are compared with two separate-effect experiments. The comparison between results obtained with the Cr-solubility model implemented in SCIANTIX and experimental data by Riglet-Martial et al. is presented in Fig. 6. The added value of the optimized model compared to the standard one is the capability of reproducing the rapid decrease in chromium content. In contrast, the calculated results have a different trend in the high-temperature region (purple colour in Fig. 6); this can be attributed to the fact that the optimized laws have a monotonic trend in temperature.

[3] Given that the system is near-stoichiometric and the electron-hole formation energy is much smaller than the oxygen Frenkel energy, the formation of couples $[e^-] = [h^+]$ should be the major charge balance mechanism. However, due to the high temperature regime considered, the formation of Frenkel defects still has an impact on diffusion mechanisms and, in this approximation, it is considered as the main mechanism.

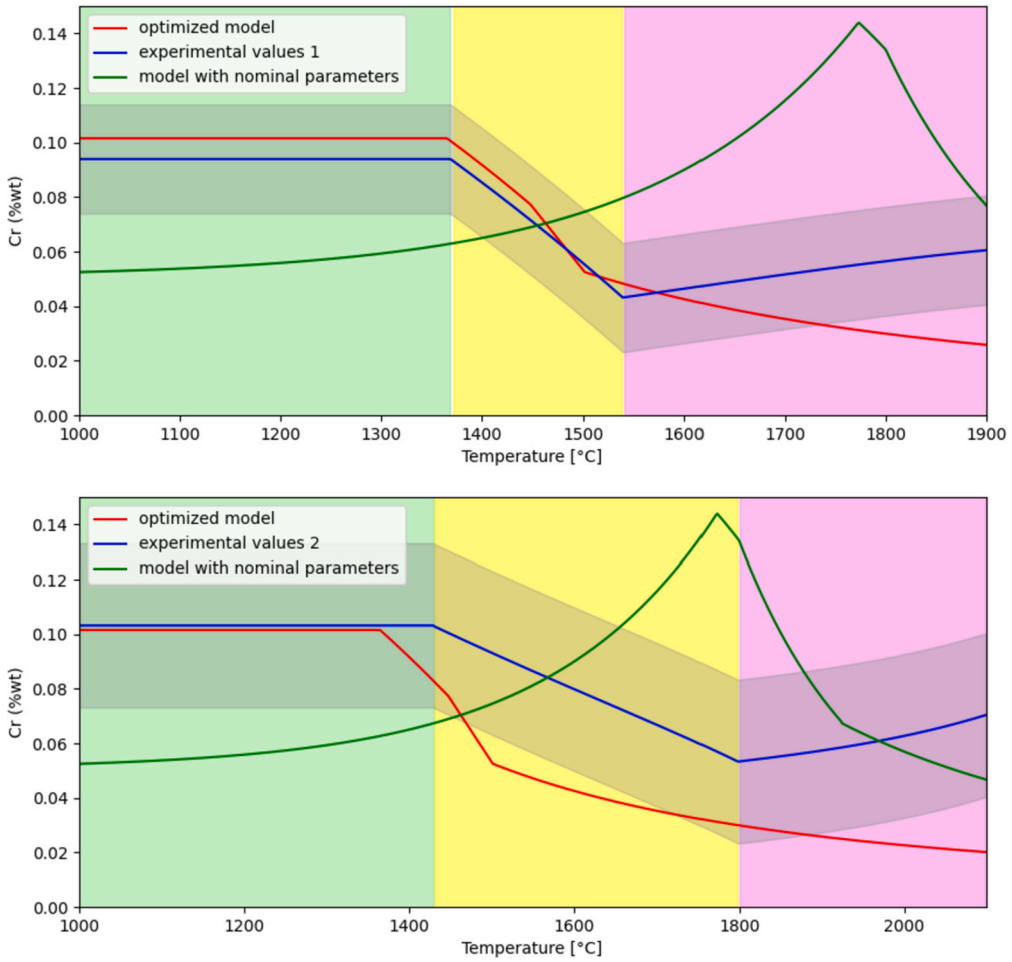

Fig. 6. Comparison between the experimental data from the work by Riglet-Martial and coauthors [16], in blue, results obtained with the optimized model, in red and results obtained from the model with nominal parameters, in green. Three regions are highlighted: the green one, representing the area in which chromium solubility is independent of the temperature, the yellow one, in which a sudden decrease of the chromium in the lattice is observed, and the violet one, where an increase in the chromium content is observed. The grey area represents the uncertainty related to the dispersed experimental data. Note that data related to experiment 1 stops at a lower temperature, due to different experimental conditions.

In addition, results obtained with the new model for the diffusion coefficient implemented in SCIANTIX are compared with FGR experimental data by Killeen [31].

The author considered six small cylindrical samples, 2.1 mm diameter by 10 mm long, prepared with 2% enriched UO_2 pellets by cutting and centreless grinding. Three of the samples were undoped and the other three were prepared from material that had been sintered using 0.5 wt% (5000 ppm) of Cr_2O_3 as a dopant. Both sets of samples were prepared from the same original batch of UO_2 powder, the dopant being added only to one portion of this material.

The grain size obtained at the end of the process was 6 μm for the undoped sample while for the doped one is in the interval 50 - 55 μm. Samples were electrically heated at a nominal temperature of 1460 °C and irradiated in a neutron flux of 3.3 $\cdot 10^{17}$ n m^{-2} s^{-1}. The samples were irradiated in pairs, with a reference sample and one doped sample in each pair, to three differing burnups, 0.14% FIMA, 0.30% FIMA, and 0.45% FIMA. After irradiation, the quantity of ^{85}Kr released into the capsules from each specimen was measured.

The comparison between the results obtained with the new diffusion coefficient and the experimental data is shown in Fig. 7, showing good agreement in the results. It should be understood in a purely qualitative sense because of the limited experimental data and the high uncertainty of the diffusion coefficient.

In addition, it may be noticed that the FGR calculated in SCIANTIX is zero up to a certain threshold. This behaviour is related to the inter-

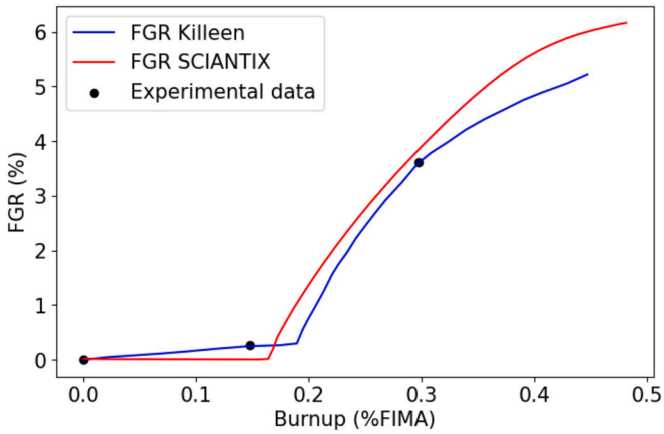

Fig. 7. Comparison of FGR values obtained with the diffusion coefficient derived in this work, in red, experimental values, represented with black dots, and their interpolation, in blue [31].

granular fission gas model implemented in SCIANTIX, which causes the gas arriving from the grains to accumulate at the grain boundary until a threshold value of fractional coverage is reached [30]. A further improvement may come from the implementation of a model for the athermal release, accounting for a partial release before saturation in grain boundary [45].

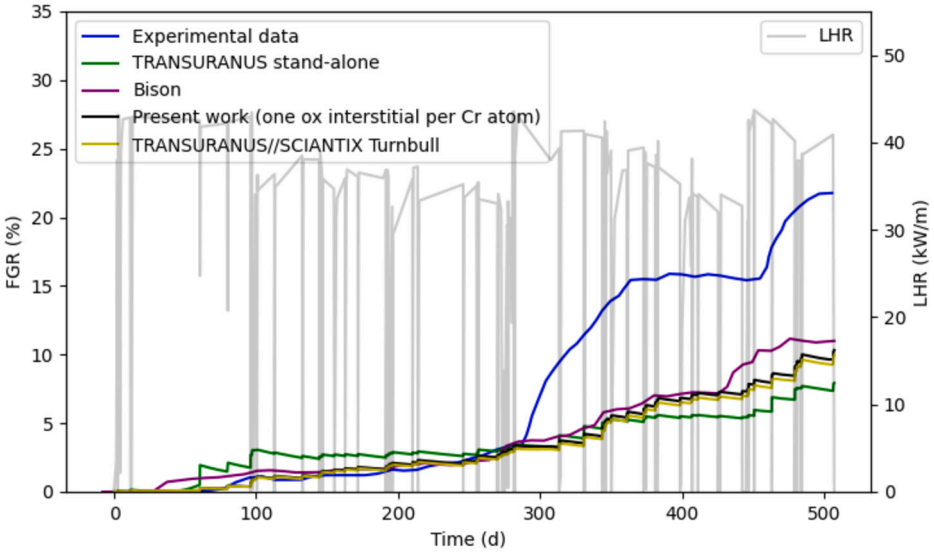

Fig. 8. Comparison between FGR as a function of rod irradiation time for IFA-677.1 Rod 1: in blue the experimental data, in black results obtained in this work with TRANSURANUS coupled with SCIANTIX considering the new diffusion coefficient for gas diffusion, in yellow results obtained with TRANSURANUS coupled with SCIANTIX using the diffusion coefficient by Turnbull [33], in green results obtained with TRANSURANUS stand-alone, and in purple results obtained with BISON from the work by Cooper and coauthors [27]. The Linear Heat Rate values are also reported, in light grey, in the background.

Table 2
Fabrication characteristics of IFA-677.1 Rod 1.

	IFA-677.1 Rod 1
Cladding material	Zircaloy-4
Fuel material	UO_2 with additives
Fill gas	He
Total rod length (mm)	456.0
Total active fuel stack length (mm)	398.6
Drilled active section length, top (mm)	109.2
Drilled active section length, bottom (mm)	109.7
Pellet inner diameter, drilled sections (mm)	1.8
Pellet outer diameter (mm)	9.13
Diametral gap (μ)	170
Cladding thickness (mm)	0.725
Cladding outer diameter (mm)	10.75
Free volume (cm^3)	5.34
Fill gas pressure (MPa)	1.35
Fuel Cr_2O_3 content (ppm)	900
Fuel Al_2O_3 content (ppm)	200
Fuel U-235 enrichment (%)	4.94
Initial fuel density (kg/m^3)	10690
Fuel average grain radius (μm)	28

3.2. Integral assessment

Few experimental data regarding chromium-doped fuel are available in the literature. In the following it is presented the description of Rod 1 from the Instrumented Fuel Assembly (IFA) 677 that was irradiated in the OECD Halden Boiling Water Reactor (HBWR) [46].

The High Initial Rating Test IFA-677.1 was performed with the aim of investigating the performance of modern fuels subjected to high initial rating with respect to thermal behaviour, dimensional changes (densification and swelling), FGR, and PCMI. All rods were instrumented with pressure transducers and fuel centreline thermocouples on both ends. The test was loaded in the HBWR in December 2004 and completed six cycles of irradiation under HBWR conditions in September 2007, achieving a rig average burnup of ~ 26.3 MWd/kgUO_2.

IFA-677.1 Rod 1 contains UO_2 doped with 900 ppm of Cr_2O_3 and 200 ppm of Al_2O_3. Fabrication characteristics of the rod considered in this work are illustrated in Table 2 [47] [48].

The new model for the gas diffusion coefficient has been fully implemented in SCIANTIX [19]. SCIANTIX receives input temperature history, fission rate, fuel hydrostatic stress, and fabrication data, then performs a 0D simulation of the fuel behaviour. The comparison of the predicted gas releases with the experimental results is crucial to assess the accuracy of the model. Results obtained with TRANSURANUS stand-alone and TRANSURANUS coupled with SCIANTIX are also shown, highlighting the added value of SCIANTIX models.

The calculated FGR as a function of rod irradiation time is shown in Fig. 8 along with the measured data (which are inferred from the inner rod pressure on-line measurement) and with BISON prediction [49], that are present as a comparison.

One can clearly see the contribution of SCIANTIX models, which allow for a more physical description of FGB, with sudden increases in conjunction with power ramps. This is possible through different models for intra-granular gas diffusion, with different trapping, resolution rates [50], and intra-granular bubble evolution [51] and grain boundary microcracking [52]. Thus, results obtained with TRANSURANUS coupled with SCIANTIX are considered as references and are described in the following.

FGR is well predicted during the first 300 days, which corresponds to a burnup of ~17 MWd/KgU. After that, FGR is underpredicted, with the calculated value at the end of life being 10.3% and the experimental value being 22%.

As a comparison, BISON underpredicts less during irradiation but reaches a similar value after the last cycle. Two main spikes in the FGR behaviour are identified in correspondence of the two power ramps, in the simulation they are present qualitatively but there is a discrepancy of up to a factor 2, which can be considered acceptable, given the inherent modelling uncertainties for FGR [38].

4. Discussion

The previous section showcased simulations of separate-effect experiments and an integral case. The results obtained through EPMA in the work by Riglet-Martial at al. [16], which are used to optimize the Cr-solubility and phase evolution models, can be well reproduced by the new model. However, this approach is limited and does not allow a proper understanding and description of the behaviour of chromium in the UO_2 lattice during irradiation.

To address these limitations, the implementation of a surrogate model for describing the Cr-U-O phase diagram, obtained through CALPHAD calculations [53], is a future development of potential interest for the SCIANTIX code.

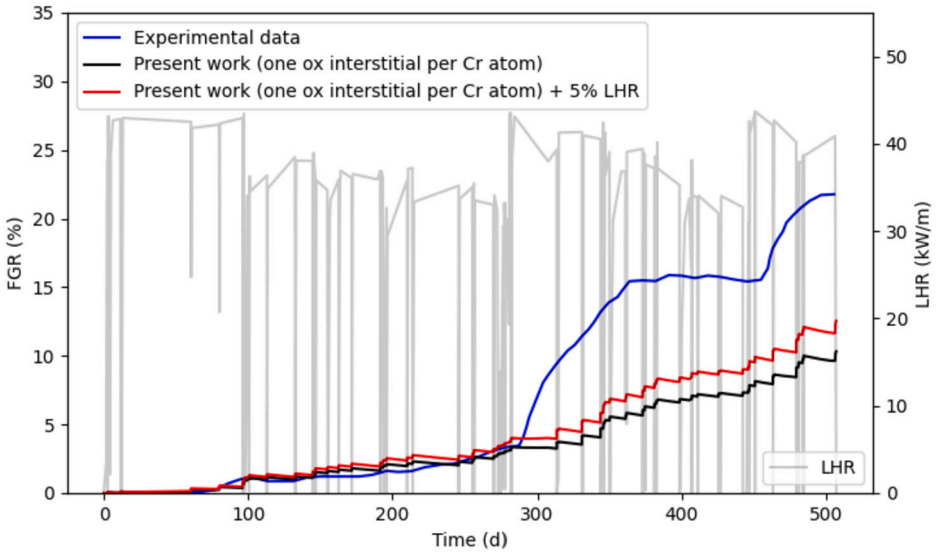

Fig. 9. Comparison between FGR as a function of rod irradiation time for IFA-677.1 Rod 1: in blue the experimental data, in black results obtained in this work with TRANSURANUS coupled with SCIANTIX considering the new diffusion coefficient for gas diffusion, in red results obtained increasing the LHR by 5%. The Linear Heat Rate values are also reported, in light grey, in the background.

Regarding the experimental results obtained by Killeen [31], since the sample considered in this experiment was doped with a large amount of chromium (5000 ppm), well above the solubility limit, there might be an effect of reduced intergranular diffusion, due to chromium precipitations at grain boundaries. This could explain why the model predictions are slightly higher than the experimental data.

The key aspect that one is able to capture, going from a simulation with standard-size fuel grains ($\sim 5-7$ μm) to one with bigger-size grains (~ 50 μm), is that the FGR begins later and continues more gently during the irradiation time. This is explained by the lower surface-to-volume ratio $\frac{S}{V}$: saturation at grain boundaries occurs earlier, due to the presence of fewer grain boundaries, as a direct result of larger grains. Thus, grain boundaries are less able to store FGs in fuel with bigger grains.

At the same time, this is counterbalanced by the greater distance to travel for each gas atom, which causes the release to proceed at a slower rate, ultimately leading to greater retention of FGs, resulting in reduced pressure in the fissure/plenum but greater gaseous swelling.

For what concerns the integral assessment, it can be seen that the impact of the new model is limited on the overall fuel performance analysis,[4] but it paves the way for a more refined analysis of the diffusivity variation (e.g., by using defect balance equation or through an evaluation of the microstructure of the doped fuel from the complete phase diagram analysis).

In addition, downstream of a sensitivity analysis, the discrepancy in the FGR results can not be explained by uncertainty on input quantities. As an example, a typical factor of uncertainty in power in the Halden reactor was considered (5%) and results obtained are shown in Fig. 9. One can clearly see that this uncertainty factor for the power is not sufficient to influence FGR results. The explanation for this discrepancy is to be found in the physical models describing the behaviour of gas in the fuel, in the uncertainty about the diffusion coefficient, and in the possible decreased capability of grain boundaries to store fission gas due to the presence of chromium precipitates at grain boundaries.

[4] Note that only the diffusion coefficient that considers one oxygen atom in interstitial position per Chromium atom in the lattice is plotted, as more consistent with the results obtained in the experimental work by Murphy et al., [18].

5. Conclusions

Chromium-doped fuels are among the most promising innovative nuclear fuels under investigation. As proven by the most recent developments, their main advantage is that they allow higher burnups to be achieved, due to higher fission gas retention, thanks to larger grains. Another potential advantage, which is still being investigated, includes the possible delay in developing the High Burnup Structure [54].

The current work aims to properly describe the chromium-UO_2 system relying on physics-based modelling of chromium solubility and diffusion coefficient, with a specific focus on Fission Gas Release.

An analytic formulation has been derived for the solubility of chromium in the UO_2 and a simple formulation to account for the phase evolution during irradiation. The solubility model was then optimized to reproduce the few experimental data available better, targeting the decrease in chromium content in the lattice at intermediate temperature. It should be emphasized that further developments are needed to correctly describe the behaviour of chromium in the UO_2 lattice at high temperatures.

Concerning the gas diffusivity, the standard diffusion coefficient has been modified in order to consider the effects of chromium in the lattice. An approach based on defect concentration was developed. All proposed models were implemented in the mesoscale code SCIANTIX.

The consistency of each model has been verified separately with experimental data, and a preliminary integral assessment has been carried out. The results of the comparison with experimental data highlight the fundamental behaviour of a fuel with large grains: an earlier release is observed, due to faster grain-boundary saturation, despite the lower overall release values, consistent with the longer gas diffusion distance.

The FGR results show a discrepancy with respect to experimental data comparable with the typical uncertainties associated with FGR, which is the combination of different phenomena. Further work is needed, for example to examine in more detail the potential changes at the grain boundaries or the grain growth and restructuring in high burnup fuel doped with Cr. Moreover, a lack of knowledge about some specific behaviours of the dopants may be overcome through new experiments to evaluate the dopant effect on fuel property.

CRediT authorship contribution statement

Giovanni Nicodemo: Writing – original draft, Software, Investigation. **Giovanni Zullo:** Writing – review & editing, Software. **Fabiola**

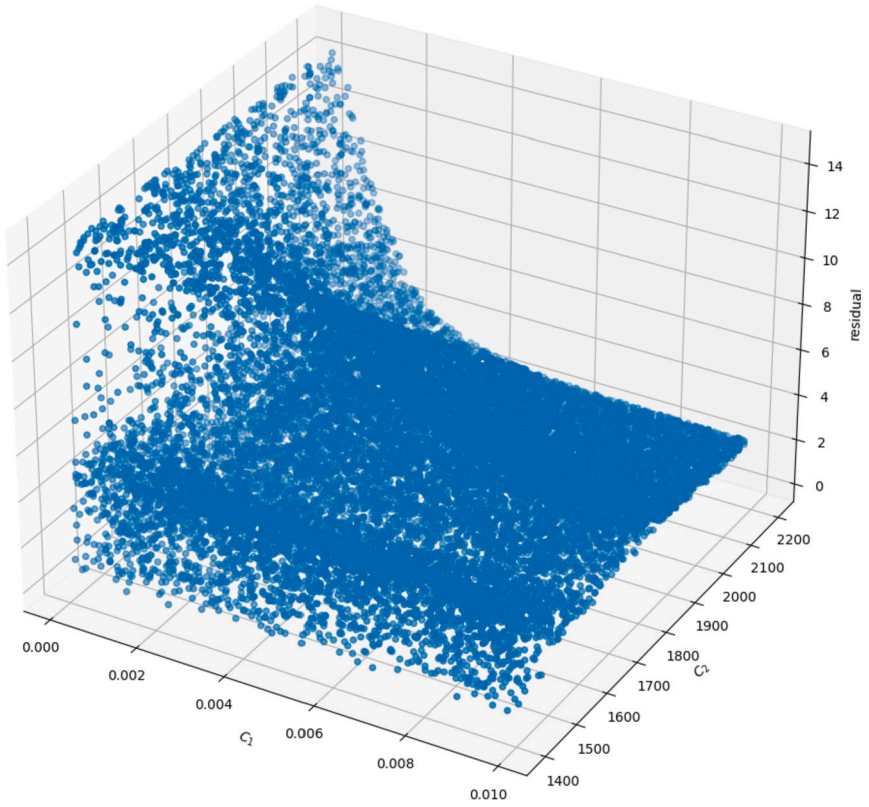

Fig. A.10. Map of C_1 and C_2 coefficients with respect to the residual.

Cappia: Writing – review & editing, Investigation. **Paul Van Uffelen:** Writing – review & editing, Writing – original draft, Supervision. **Alejandra De Lara:** Writing – review & editing, Software, Investigation. **Lelio Luzzi:** Writing – review & editing, Supervision, Resources, Project administration, Funding acquisition. **Davide Pizzocri:** Writing – review & editing, Validation, Supervision, Conceptualization.

Declaration of competing interest

The authors declare that they have no known competing financial interests or personal relationships that could have appeared to influence the work reported in this paper.

Data availability

Data will be made available on request.

Acknowledgements

This project has received funding from the Euratom research and training programme 2021–2027 through the OperaHPC project under grant agreement n° 101061453. Views and opinions expressed in this paper reflect only the authors' view and the Commission is not responsible for any use that may be made of the information it contains.

Appendix A. Optimization of Cr-solubility model

The optimization process carried out for the solubility model and Cr phase evolution during irradiation refers to 5 parameters. Since chromium solubility in the lattice was derived to be

$$\log_{10}(y_{Cr}) = q\,\log_{10}(P_{O_2}) + V + \frac{U}{T} \tag{A.1}$$

and experimentally it was found that solubility is a fixed quantity below a certain temperature. Thus the parameters selected are U, V, and T_{max}, representing the temperature beyond which the solubility starts to behave according to Eq. (A.1). Regarding the evolution of the phases during irradiation, it was described according to the following formula

$$f(T) = 1 - \exp(C_1(T - C_2)) \tag{A.2}$$

Hence, the other two parameters selected are C_1 and C_2. The optimization process is performed by random sampling values of the parameters in ranges centred around their nominal value. The number of trials is 10000 in order to have good statistics. The results in terms of chromium content in the lattice are compared with experimental data, considering the difference normalized by the nominal value, and the best coefficients are chosen. Representative maps are shown in Fig. A.10, Fig. A.11, and Fig. A.12. Local minimum can be identified for the first two maps, evidencing the fact that there are specific parameters that minimize the error with respect to the experimental data, while in Fig. A.12 it can be seen that the results are not influenced by the values of T_{max}. This is reasonable since this parameter simply shifts the point at which the solubility model itself starts acting.

The final values used in the model implemented in SCIANTIX, compared with nominal values, are reported in Table A.3. Note that only one nominal value is given in the table, although in reality, there would be two since there are two phases. However, for simplicity, the optimization was done considering only one phase.

Table A.3
Parameters value obtained from the optimization process compared with nominal ones.

Quantity	Nominal values	Optimized values
U (J/mol)	28160	22989.0
V (J/K mol)	-6.0760	-5.9483
T_{max} (°C)	1500	1448
C_1 (-)	0.0050	0.0017
C_2 (-)	1800	1502

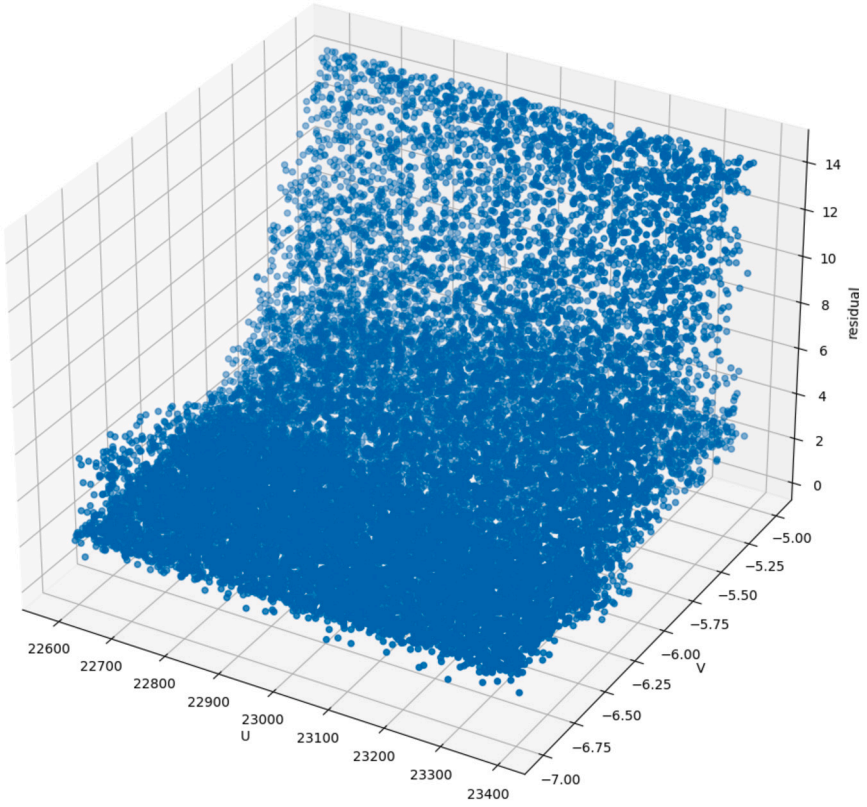

Fig. A.11. Map of U and V coefficients with respect to the residual.

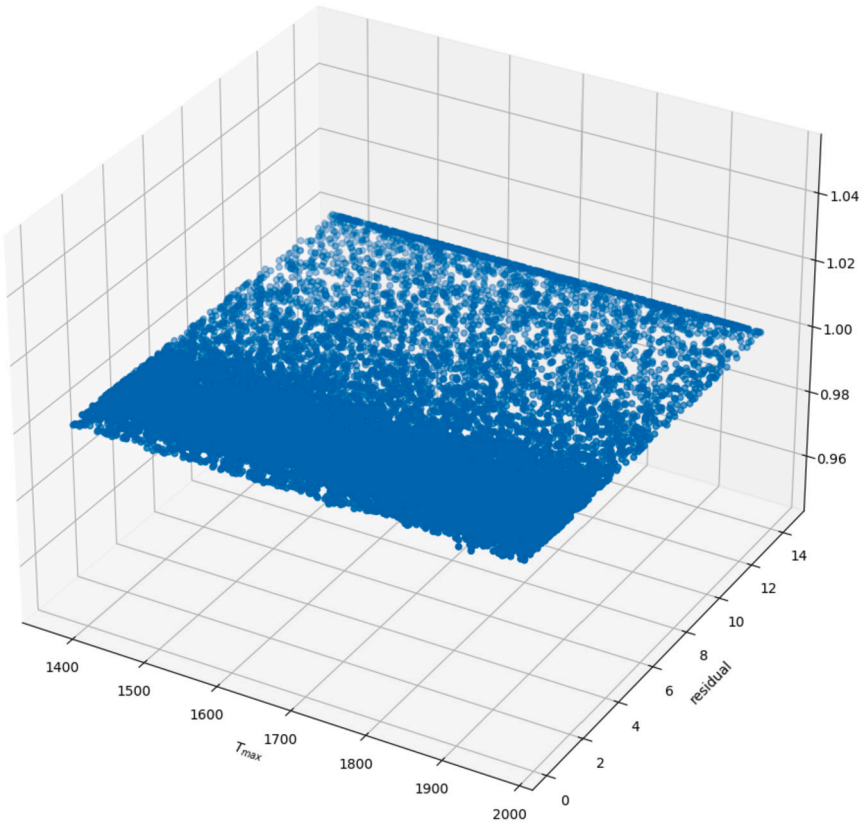

Fig. A.12. Map of T_{max} coefficient with respect to the residual.

References

[1] K.J. Geelhood, Fuel Performance Considerations and Data Needs for Burnup above 62 GWd/MTU, 2019.

[2] D.R. Olander, A.T. Motta, Light Water Reactor Materials Volume I: Fundamentals, American Nuclear Society, 2017.

[3] P. Van Uffelen, J. Hales, W. Li, G. Rossiter, R. Williamson, A review of fuel performance modelling, J. Nucl. Mater. 516 (2019) 373–412, https://doi.org/10.1016/j.jnucmat.2018.12.037.

[4] V.I. Tarasov, V.D. Ozrin, M.S. Veshchunov, Simulation of radioactive fission gas release from defective PWR fuel rod using the MFPR/R mechanistic code, J. Nucl. Mater. 583 (2023) 154536, https://doi.org/10.1016/J.JNUCMAT.2023.154536.

[5] F. Cappia, D. Pizzocri, A. Schubert, P. Van Uffelen, G. Paperini, D. Pellottiero, R. Macián-Juan, V.V. Rondinella, Critical assessment of the pore size distribution in the rim region of high burnup UO_2 fuels, J. Nucl. Mater. 480 (2016) 138–149, https://doi.org/10.1016/J.JNUCMAT.2016.08.010.

[6] D. Pizzocri, F. Cappia, L. Luzzi, G. Pastore, V.V. Rondinella, P. Van Uffelen, A semi-empirical model for the formation and depletion of the high burnup structure in UO_2, J. Nucl. Mater. 487 (2017) 23–29, https://doi.org/10.1016/j.jnucmat.2017.01.053.

[7] R.J. White, M.O. Tucker, A new fission-gas release model, J. Nucl. Mater. 118 (1983) 1–38, https://doi.org/10.1016/0022-3115(83)90176-9.

[8] S. Kashibe, K. Une, Effect of additives (Cr_2O_3, Al_2O_3, SiO_2, MgO) on diffusional release of ^{133}Xe from UO_2 fuels, J. Nucl. Mater. 254 (1998) 234–242, https://doi.org/10.1016/S0022-3115(97)00356-5.

[9] J. Arborelius, K. Backman, L. Hallstadius, M. Limbäck, J. Nilsson, B. Rebensdorff, G. Zhou, K. Kitano, R. Lofstrom, G. Ronnberg, Advanced doped UO_2 pellets in LWR applications, J. Nucl. Sci. Technol. 43 (2006) 967–976, https://doi.org/10.1080/18811248.2006.9711184.

[10] C.M. Silva, R.D. Hunt, K.S. Holliday, An evaluation of tri-valent oxide (Cr_2O_3) as a grain enlarging dopant for UO_2 nuclear fuels fabricated under reducing environment, J. Nucl. Mater. 553 (2021) 153053, https://doi.org/10.1016/J.JNUCMAT.2021.153053.

[11] M. Piro, D. Sunderland, S. Livingstone, J. Sercombe, W. Revie, A. Quastel, K. Terrani, C. Judge, A review of Pellet–Clad interaction behavior in zirconium alloy fuel cladding, https://doi.org/10.1016/B978-0-12-803581-8.09799-X, 2017.

[12] L. Bourgeois, P. Dehaudt, C. Lemaignan, A. Hammou, Factors governing microstructure development of Cr_2O_3-doped UO_2 during sintering, J. Nucl. Mater. 297 (2001) 313–326, https://doi.org/10.1016/S0022-3115(01)00626-2.

[13] J.E. Lindbäck, Advanced Fuel Pellet Materials and Designs for Water Cooled Reactors, IAEA, 2003.

[14] S.C. Middleburgh, S. Dumbill, A. Qaisar, I. Vatter, M. Owen, S. Vallely, D. Goddard, D. Eaves, M. Puide, M. Limbäck, W.E. Lee, Enrichment of chromium at grain boundaries in chromia doped UO_2, J. Nucl. Mater. 575 (2023) 154250, https://doi.org/10.1016/J.JNUCMAT.2023.154250.

[15] C. Riglet-Martial, P. Martin, D. Testemale, C. Sabathier-Devals, G. Carlot, P. Matheron, X. Iltis, U. Pasquet, C. Valot, C. Delafoy, R. Largenton, Thermodynamics of chromium in UO_2 fuel: a solubility model, J. Nucl. Mater. 447 (2014) 63–72, https://doi.org/10.1016/J.JNUCMAT.2013.12.021.

[16] C. Riglet-Martial, J. Sercombe, J. Lamontagne, J. Noirot, I. Roure, T. Blay, L. Desgranges, Experimental evidence of oxygen thermo-migration in PWR UO_2 fuels during power ramps using in-situ oxido-reduction indicators, J. Nucl. Mater. 480 (2016) 32–39, https://doi.org/10.1016/J.JNUCMAT.2016.07.056.

[17] E. Curti, D.A. Kulik, Oxygen potential calculations for conventional and cr-doped UO_2 fuels based on solid solution thermodynamics, J. Nucl. Mater. 534 (2020) 152140, https://doi.org/10.1016/J.JNUCMAT.2020.152140.

[18] G. Murphy, R. Gericke, S. Gilson, E. Bazarkina, A. Rossberg, P. Kaden, R. Thümmler, M. Klinkenberg, M. Henkes, P. Kegler, V. Svitlyk, J. Marquardt, T. Lender, C. Hennig, K. Kvashnina, N. Huittinen, Deconvoluting cr states in cr-doped UO_2 nuclear fuels via bulk and single crystal spectroscopic studies, Nat. Commun. 14 (2023), https://doi.org/10.1038/s41467-023-38109-0.

[19] D. Pizzocri, T. Barani, L. Luzzi, Sciantix: a new open source multi-scale code for fission gas behaviour modelling designed for nuclear fuel performance codes, J. Nucl. Mater. 532 (2020) 152042, https://doi.org/10.1016/J.JNUCMAT.2020.152042.

[20] A. Magni, A.D. Nevo, L. Luzzi, D. Rozzia, M. Adorni, A. Schubert, P. Van Uffelen, The TRANSURANUS Fuel Performance Code, in: Nuclear Power Plant Design and Analysis Codes: Development, Validation, and Application, 2021, pp. 161–205.

[21] G. Zullo, D. Pizzocri, L. Luzzi, F. Kremer, R. Dubourg, A. Schubert, P. Van Uffelen, Towards simulations of fuel rod behaviour during severe accidents by coupling TRANSURANUS with SCIANTIX and MFPR-F, Ann. Nucl. Energy 190 (2023) 109891, https://doi.org/10.1016/J.ANUCENE.2023.109891.

[22] E. Povoden, A.N. Grundy, L.J. Gauckler, Thermodynamic reassessment of the Cr-O system in the framework of solid oxide fuel cell (SOFC) research, J. Phase Equilibria Diffus. (2006).

[23] K. Une, S. Kashibe, K. Ito, Fission gas behavior during postirradiation annealing of large grained UO_2 fuels irradiated to 23 GWd/t, J. Nucl. Sci. Technol. (1992) 221–231.

[24] V.D. Ozrin, A model for evolution of oxygen potential and stoichiometry deviation in irradiated UO_2 fuel, J. Nucl. Mater. 419 (2011) 371–377, https://doi.org/10.1016/J.JNUCMAT.2011.06.042.

[25] M.S. Veshchunov, R. Dubourg, V.D. Ozrin, V.E. Shestak, V.I. Tarasov, Mechanistic modelling of urania fuel evolution and fission product migration during irradiation and heating, J. Nucl. Mater. 362 (2007) 327–335, https://doi.org/10.1016/J.JNUCMAT.2007.01.081.

[26] H. Kleykamp, The chemical state of the fission products in oxide fuels, J. Nucl. Mater. 131 (1985) 221–246, https://doi.org/10.1016/0022-3115(85)90460-X.

[27] M.W. Cooper, G. Pastore, Y. Che, C. Matthews, A. Forslund, C.R. Stanek, K. Shirvan, T. Tverberg, K.A. Gamble, B. Mays, D.A. Andersson, Fission gas diffusion and release for Cr_2O_3-doped UO_2: from the atomic to the engineering scale, J. Nucl. Mater. 545 (2021) 152590, https://doi.org/10.1016/J.JNUCMAT.2020.152590.

[28] G. Pastore, D. Pizzocri, C. Rabiti, T. Barani, P. Van Uffelen, L. Luzzi, An effective numerical algorithm for intra-granular fission gas release during non-equilibrium trapping and resolution, J. Nucl. Mater. 509 (2018) 687–699, https://doi.org/10.1016/j.jnucmat.2018.07.030.

[29] M.V. Speight, A calculation on the migration of fission gas in material exhibiting precipitation and re-solution of gas atoms under irradiation, Nucl. Sci. Eng. 37 (1969) 180–185, https://doi.org/10.13182/NSE69-A20676.

[30] G. Pastore, L. Luzzi, V. Di Marcello, P. Van Uffelen, Physics-based modelling of fission gas swelling and release in UO_2 applied to integral fuel rod analysis, Nucl. Eng. Des. 256 (2013) 75–86, https://doi.org/10.1016/j.nucengdes.2012.12.002.

[31] J.C. Killeen, Fission gas release and swelling in UO_2 doped with Cr_2O_3, J. Nucl. Mater. 88 (1980) 177–184, https://doi.org/10.1016/0022-3115(80)90272-X.

[32] J.A. Turnbull, C.A. Friskney, J.R. Findlay, F.A. Johnson, A.J. Walter, The diffusion coefficients of gaseous and volatile species during the irradiation of uranium dioxide, J. Nucl. Mater. 107 (1982) 168–184, https://doi.org/10.1016/0022-3115(82)90419-6.

[33] J. Turnbull, R. White, C. Wise, The diffusion coefficient for fission gas atoms in uranium dioxide, 1989.

[34] Y.S. Kim, Fission gas release from UO_{2+x} in defective fuel rods, Nucl. Technol. 130 (2000) 9–17, https://doi.org/10.13182/NT00-A3073.

[35] R.E. Carter, K.W. Lay, Surface-controlled oxidation-reduction of UO_2, J. Nucl. Mater. 36 (1970) 77–86, https://doi.org/10.1016/0022-3115(70)90063-2.

[36] A. Massih, UO_2 fuel oxydation and fission gas release, 2018.

[37] H.J. Matzke, Gas release mechanisms in UO_2—a critical review, Radiat. Eff. 53 (1980) 219–242, https://doi.org/10.1080/00337578008207118.

[38] G. Pastore, L.P. Swiler, J.D. Hales, S.R. Novascone, D.M. Perez, B.W. Spencer, L. Luzzi, P. Van Uffelen, R.L. Williamson, Uncertainty and sensitivity analysis of fission gas behavior in engineering-scale fuel modeling, J. Nucl. Mater. 456 (2015) 398–408, https://doi.org/10.1016/J.JNUCMAT.2014.09.077.

[39] M. Lyons, R. Boyle, J. Davies, V. Hazel, T. Rowland, UO_2 properties affecting performance, Nucl. Eng. Des. 21 (1972) 167–199, https://doi.org/10.1016/0029-5493(72)90072-6.

[40] M. Oguma, Cracking and relocation behavior of nuclear fuel pellets during rise to power, 76 (1) (1983).

[41] A. Massih, L. Jernkvist, Effect of additives on self-diffusion and creep of UO_2, Comput. Mater. Sci. 110 (2015) 152–162, https://doi.org/10.1016/j.commatsci.2015.08.005.

[42] A. Massih, L. Jernkvist, Effects of additives on UO_2 fuel behavior: expanded edition, 2021.

[43] J.B. Ainscough, B.W. Oldfield, J.O. Ware, Isothermal grain growth kinetics in sintered UO_2 pellets, J. Nucl. Mater. 49 (1973) 117–128, https://doi.org/10.1016/0022-3115(73)90001-9.

[44] P. Van Uffelen, P. Botazzoli, L. Luzzi, S. Bremier, A. Schubert, P. Raison, R. Eloirdi, M.A. Barker, An experimental study of grain growth in mixed oxide samples with various microstructures and plutonium concentrations, J. Nucl. Mater. 434 (2013) 287–290, https://doi.org/10.1016/J.JNUCMAT.2012.11.053.

[45] P. Van Uffelen, Modelling the influence of the athermal open porosity on fission gas release in LWR fuel, 2002.

[46] mooseframework.inl.gov/bison/LWR/validation/IFA_677/doc/IFA-677.html.

[47] R. Jošek, The High Initial Rating Test IFA-677: Final Report on In-Pile Results, Technical Report HWR-872, OECD Halden Reactor Project, 2008.

[48] H.K. Jenssen, PIE Report on Six UO_2 Fuel Rods Irradiated in IFA-677 High Initial Rating Test, Technical Report HWR-968, OECD Halden Reactor Project, 2010.

[49] Y. Che, G. Pastore, J. Hales, K. Shirvan, Modeling of Cr_2O_3-doped UO_2 as a near-term accident tolerant fuel for lwrs using the bison code, Nucl. Eng. Des. 337 (2018) 271–278, https://doi.org/10.1016/J.NUCENGDES.2018.07.015.

[50] P. Lösönen, Calculation method for diffusional gas release with grain boundary resolution, Nucl. Eng. Des. 201 (2000) 139–153, https://doi.org/10.1016/S0029-5493(00)00295-8.

[51] D. Pizzocri, G. Pastore, T. Barani, A. Magni, L. Luzzi, P. Van Uffelen, S.A. Pitts, A. Alfonsi, J.D. Hales, A model describing intra-granular fission gas behaviour in oxide fuel for advanced engineering tools, J. Nucl. Mater. 502 (2018) 323–330, https://doi.org/10.1016/J.JNUCMAT.2018.02.024.

[52] T. Barani, E. Bruschi, D. Pizzocri, G. Pastore, P. Van Uffelen, R.L. Williamson, L. Luzzi, Analysis of transient fission gas behaviour in oxide fuel using BISON and TRANSURANUS, J. Nucl. Mater. 486 (2017) 96–110, https://doi.org/10.1016/J.JNUCMAT.2016.10.051.

[53] H.L. Lukas, S.G. Fries, B. Sundman, Frontmatter, computational thermodynamics: the calphad method, https://api.semanticscholar.org/CorpusID:116751125, 2007.

[54] D. Baron, M. Kinoshita, P. Thevenin, R. Largenton, Discussion about HBS transformation in high burn-up fuels, Nucl. Eng. Technol. 41 (2009), https://doi.org/10.5516/NET.2009.41.2.199.